

Article

One-Step Synthesis of Silver Nanoparticles Using Saudi Arabian Desert Seasonal Plant *Sisymbrium irio* and Antibacterial Activity against Multidrug-Resistant Bacterial Strains

Suresh Mickymaray

Department of Biology, College of Science, Al-Zulfi-, Majmaah University, Majmaah 11952, Riyadh Region, Saudi Arabia; s.maray@mu.edu.sa or drsuresh.maray@gmail.com; Tel.: +966-582-315-293

Received: 28 September 2019; Accepted: 27 October 2019; Published: 28 October 2019



Abstract: Globally, antimicrobial resistance has grown at an alarming rate. To combat the multidrug-resistant (MDR) superbugs, silver nanoparticles (Ag NPs) were synthesized using an aqueous leaf extract of seasonal desert plant *Sisymbrium irio* obtained from the central region of Saudi Arabia by a simple one-step procedure. The physical and chemical properties of the Ag NPs were investigated through ultraviolet visible analysis (UV-vis), Fourier-transform infrared (FTIR) spectroscopy, X-ray diffraction (XRD), scanning electron microscope (SEM), and transmission electron microscope (TEM) analysis. The UV-vis spectrum showed an absorption band at 426 nm. The XRD results showed a highly crystalline face-centered cubic structure. The surface morphology analyzed using SEM and TEM analyses showed the particle size to be in the range 24 nm to 50 nm. Various concentrations of Ag NPs were tested against MDR *Pseudomonas aeruginosa* and *Acinetobacter baumannii* that cause ventilator-associated pneumonia (VAP). American Type Culture Collection (ATCC) *Escherichia coli*-25922 was used as the reference control strain. The Ag NPs effectively inhibited tested pathogens, even at the lowest concentration (6.25 µg) used. The bacterial inhibitory zone ranged from 11–21 mm. In conclusion, the newly synthesized Ag NPs could be a potential alternative candidate in biomedical applications in controlling the spread of MDR pathogens.

Keywords: *Sisymbrium irio*; silver nanoparticles; characterization; ventilator-associated MDR pathogens; antibacterial activity

1. Introduction

For the past two decades, the interest in the synthesis of ecofriendly metal and metal oxide nanoparticles has grown dramatically in the research fields of material science and engineering and biotechnology. Because of the high ‘surface-to-volume ratio’ of the nanoparticles, they have unique properties of size, shape, self-assembly, and conductivity. Among the widely studied silver (Ag) [1], gold (Au) [2], platinum (Pt) [3], and palladium (Pd) [4] nanoparticles, Ag NPs have gained much attention due to their various applications in gas sensors [5], dye-sensitized solar cells [6], textiles [7], water purification systems [8], cosmetics [9], and food packaging [10]. They show antimicrobial [11], larvicidal [12], anti-cancer, dye degrading [13], and antibiofilm forming [1] properties. Conventional methods of synthesis of nanoparticles are high cost, utilize more energy, and consume more time. The chemical reducing agents used cause environmental issues. Hence, these issues must be overcome, and actions are needed to determine an alternate method for the synthesis of nanoparticles. Generally, methods of green synthesis of nanoparticles use algae, fungi, and various lower and higher plants [12]. Plant-based synthesis is more convenient than microbial method since the latter suffers from the high cost of culture media, time consumption for growth enhancement, difficulty in handling the process,

and requirement of biological knowledge. Usually, different plant parts, such as the leaf, bark, root, stem, seed, flower, fruit, and tubers, have been used for nanoparticle synthesis [14]. The plant materials are selected based on the content of bioactive phytoconstituents in the exact plant part through the knowledge gained from studying the literature. The leaf part of plants is preferred by many researchers for the synthesis of metal nanoparticles due to the rich content of bioactive phytoconstituents in leaves, their easy availability, and readiness for instant use [15]. The bioactive phytoconstituents act as capping, as well as reducing agents, for the synthesis of nanoparticles. Previously, several attempts have been made for the synthesis of Ag NPs using leaf extracts of plants like *Dodonaea viscosa* [11], *Gloriosa superba* [16], *Lilium lancifolium* [1], *Salvia spinosa* [17], *Mukia scabrella* [18], and *Syzygium alternifolium* [19].

Sisymbrium irio L. belongs to the family of Cruciferae. It is widely distributed in the deserts of the central region of Saudi Arabia during the winter season between January and May. It is used for dietary purposes due to its high nutrient and protein (35%) content. This plant contains several phytoconstituents like glycosides, triterpenes, amino acids, coumarin, tannins, flavonoids, alkaloids, and saponins [20,21]. The ethanol extract of seeds has shown better antibacterial, antipyretic, and analgesic activities, while the n-hexane extract of aerial parts exhibit better antibacterial and cytotoxic activities.

At present, the antimicrobial resistance-related infectious diseases, including hospital-acquired Gram-negative bacterial infection and its associated morbidity and mortality, have grown at an alarming rate. Most of the presently available antibiotics have become ineffective to treat and control the multidrug resistant bacterial pathogens globally [22–25].

The multidrug-resistant bacteria, mainly *Pseudomonas aeruginosa* and *Acinetobacter baumannii*, are the most important nosocomial pathogens in the healthcare-associated environment and cause high mortality [26–29]. The infections caused by these two species are difficult to treat because they are naturally resistant to many antibiotics and develop new resistance mechanisms continuously. Furthermore, these two bacteria can be transmitted through personal contact (direct) or contaminated environments (indirect contact) [30]. Moreover, *A. baumannii* can easily spread in hospital environments and survive for long periods [31]. For the reason, the nosocomial infections by these two pathogens have become a major health concern in many hospitals worldwide [32].

Typically, medicinal plant extracts have been used for their antibacterial potential, which is due to the presence of bioactive principles. However, the antibacterial activity of plant bioactive has some limitations, such as dependency on dosage concentration, applicability on a narrow range of bacterial species, and low stability [33]. Recently, Lim et al. reported that actinomycetes isolated from soil showed better antibacterial activity against multidrug resistant bacteria [34]. However, these methods are difficult to follow, and consume more time for growing the media. Keeping the above issues in mind, the present study explored Ag NPs synthesized by a green method for the effective growth inhibition of the multidrug resistant bacteria with low concentration.

This study demonstrated a simple methodology for the synthesis of Ag NPs using the leaves extract of *S. irio* available in the central region of Saudi Arabian deserts during the winter. The advantages of this study are: (i) Room temperature process, (ii) less time consumption (15 min), (iii) reliability, (iv) simplicity, and (v) mass production. As per the existing literature and knowledge, this is probably the first report on the synthesis of Ag NPs using *S. irio* leaves extract. The Ag NPs were characterized and the crystal structure, optical and morphological properties were investigated. The effect of different concentrations of Ag NPs was investigated against nosocomial multidrug-resistant Gram-negative bacterial strains *P. aeruginosa* and *A. baumannii* with American Type Culture Collection (ATCC) *Escherichia coli*-25922 strain as the reference. This finding may help in the field of medicinal research to control the multidrug resistant-related morbidity and mortality.

2. Materials and Methods

2.1. Chemicals

Silver nitrate (AgNO_3), Mueller Hinton Agar (MHA), and Nutrient Broth (NB) were procured from HiMedia Laboratories Pvt. Ltd (HiMedia, Mumbai, India). For all the experiments, analytical grade reagents and ultrapure water (Milli-Q) were used.

2.2. Collection of the Plant Material

The plant leaves were collected during the winter season (Location: 26.3158330N; 44.8608130E) at the College of Science, Al Zulfi campus, Kingdom of Saudi Arabia (Figure 1). The deposited voucher specimen bearing the no: 22185 can be found in the herbarium in the Botany Department of King Saud University, Riyadh, Kingdom of Saudi Arabia.



Figure 1. Saudi Arabian desert seasonal plant of *Sisymbrium irio*.

2.3. Collection of Bacterial Pathogens

The ventilator-associated pneumonia-causing multidrug-resistant *P. aeruginosa* and *A. baumannii* and the reference strain ATCC-25922 *E. coli* were obtained from the culture stock maintenance at Microbiology Laboratory, College of Science, Al Zulfi, Kingdom of Saudi Arabia.

2.4. Identification of Bacterial Strains

The bacteria were identified and their antimicrobial drug resistance was detected by VITEK 2 compact automated system using a GN: 21341 identification card and AST-N 292 antimicrobial susceptibility cards, respectively (BioMérieux, Durham, NC, USA). The bacterial pathogens resistant to more than one antibiotic were considered as multidrug-resistant. The susceptibility pattern was interpreted as per the recommendations of European Committee on Antimicrobial Susceptibility Testing (EUCAST) as shown in Table 1.

2.5. Synthesis of Ag NPs

For the preparation of aqueous leaf extract of *S. irio*, fresh leaves were collected and washed in running tap water and rinsed well with the Ultrapure Milli Q water. Then, 10 g of leaves were chopped into 1–2 cm. Cut leaf pieces were inoculated into 100 mL of Ultrapure Milli Q water in a 250-mL conical flask and boiled for 10 min. Following this, the aqueous leaf extract was filtered through Grade No.1

Whatman filter paper (125 mm). The aqueous leaf extract was collected in a conical flask and stored at room temperature (25 ± 2 °C) for further use.

About 50 mL of *S. irio* aqueous leaf extract was added to 450 mL of 1mM AgNO₃ solution and stirred at 35 °C using a magnetic stirrer. After 15 min, a yellowish-brown color was observed, indicating the formation of Ag NPs [35]. The solution containing the Ag NPs was transferred into a watch glass and incubated at 60 °C for 24 h. The solution containing Ag NPs/dry powder was used for structural, morphological, and optical characterization, as well as for assessing the antibacterial activity.

2.6. Characterization

The Ag NPs were subjected to UV-visible analysis (UV-vis, 200 nm to 800 nm) using a Shimadzu spectrophotometer (Model UV-1800, Kyoto, Japan) operating at a resolution of 1 nm. Fourier-transform infrared spectroscopic (FTIR) analysis of the nanoparticles was done using a Spectrum-65 FTIR spectrometer (PerkinElmer Co., Ltd., Waltham, MA, USA). The FTIR measurement of the sample was taken in the wavenumber region 4000 cm⁻¹ to 400 cm⁻¹ using 16 accumulated scans in the attenuated total reflection mode with diamond/ZnSe (one reflection) crystal. The structural analysis of Ag NPs was carried out using a powder X-ray diffractometer (PANalytical X'Pert Pro, PANalytical X'Pert Pro, Carnation, WA, USA) with Cu-K α radiation (wavelength:1.5418 Å) with nickel monochromator in the range of 2 θ from 10° to 80°. The nano-crystallite domain size was calculated from the width of the XRD peaks using Debye-Scherrer's formula $D = 0.9\lambda/\beta\cos\theta$ [36]. The surface topology of Ag NPs was studied by scanning electron microscope (SEM, EVO 18 SEM, Carl Zeiss, Jena, Germany). For accuracy, morphological structures and actual particle size were analyzed under transmission electron microscope (TEM, JEOL Electron Optics Laboratory, Tokyo, Japan) operated at 200 kV. To facilitate TEM analysis, a drop of solution containing the Ag NPs was dispensed to a carbon-coated 200 mesh copper grid and allowed to air-dry at room temperature just before the examination.

2.7. Antibacterial Assay

The antibacterial activity of the synthesized Ag NPs was tested against *P. aeruginosa*, *A. baumannii* with the reference strain ATCC *E. coli*-25922 by agar well diffusion method [37]. The overnight bacterial cultures were standardized using the McFarland standard (10⁶ cfu/mL). The silver nanoparticle suspension was prepared by mixing 1 mg of Ag NPs in 1 mL of distilled water (1 mg/1 mL concentration). The nanoparticle suspension was sonicated for 15 min for dispersion of the particles. Mueller–Hinton plates were prepared and each bacterial strain was spread uniformly onto the plates using spread plate technique aseptically. After spreading the bacteria, five wells of 6 mm diameter were made in each plate using a sterile cork borer. Using sterile micropipette tips, each culture plate was added with five different concentrations (6.25, 12.5, 25, 50, and 100 μ g) of the nanoparticle suspension. A standard antibiotic disc Meropenem (10 μ g) was used as a positive control. The culture plates were incubated at 37 °C for 24 h. After incubation, antibacterial activity was determined by measuring the zone of inhibition from each well and the experiment was conducted in triplicates.

2.8. Statistical Analysis

All the results were reported as mean \pm standard error of three independent biological replicates. We employed ANOVA followed by Tukey's HSD test ($p \leq 0.05$) to analyze the data from the antibacterial activity with the help of the SPSS software package 16.0 version.

3. Results

3.1. UV-Vis Spectroscopic Analysis

The *S. irio* leaf extract showed an absorption peak at 326 nm due to the $\pi \rightarrow \pi^*$ transition taking place in the plant bioactive compounds (Figure 2). The Ag NO₃ solution did not show any absorption in

the UV-vis spectrum. The reaction mixture containing AgNO₃ solution and the leaf extract monitored at 5, 10, and 15-min time intervals exhibited absorbance peak at 426 nm [16].

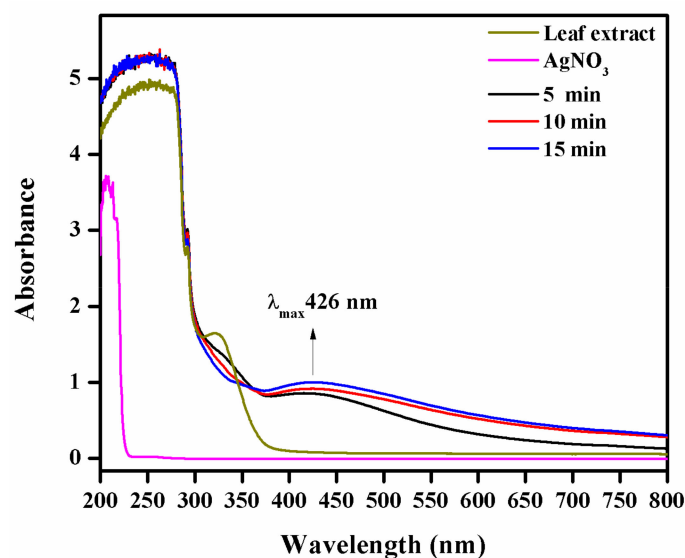


Figure 2. Ultraviolet visible (UV-vis) analysis of Ag nanoparticles (NPs).

3.2. FTIR Analysis of Synthesized Ag NPs

FTIR spectroscopy is commonly used to identify the organic and inorganic functional groups of material. The FTIR spectra of *S. irio* leaf extract and the synthesized Ag NPs are shown in Figure 3. Both the spectra showed bands at 3309, 2117, 1630, 602, and 508 cm⁻¹. The strong band at 3309 cm⁻¹ corresponds to alcoholic O-H stretching. The weak band at 2117 cm⁻¹ is owing to the C=N stretching of R-N=C=S. The sharp band at 1630 cm⁻¹ can be assigned to N-H stretching. The lower frequency bands at 602 and 508 cm⁻¹ can be assigned to N-H bending C-Cl stretching vibrations. In the IR spectrum of the Ag NPs, a new band, observed at 1337 cm⁻¹, corresponds to the -C-O stretching [38–40].

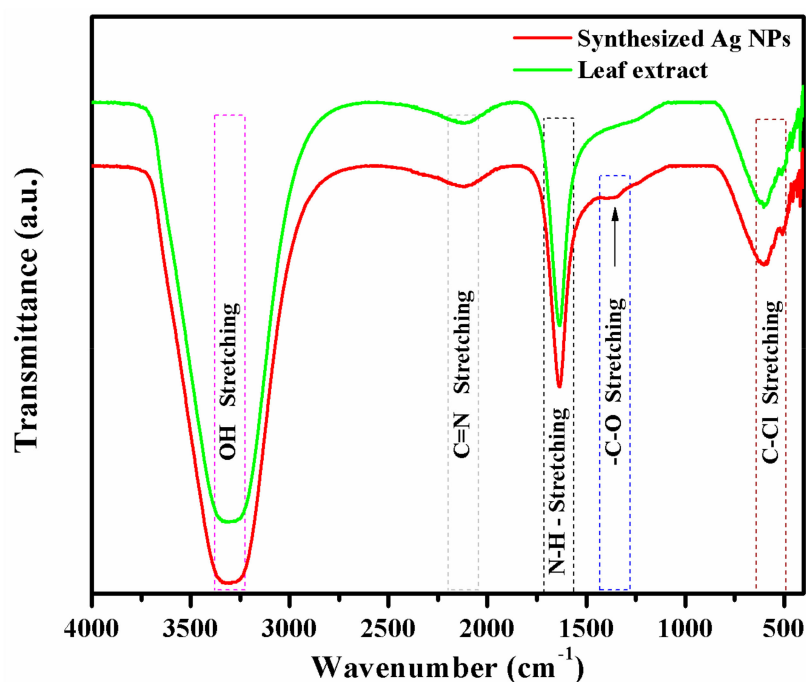


Figure 3. Fourier-transform infrared (FTIR) spectrum of leaf extract and synthesized Ag NPs.

3.3. XRD Analysis

The powder X-ray diffraction patterns revealed the nanocrystalline nature of Ag NPs as shown in Figure 4. The XRD patterns indicated four intense peaks at angles (2θ) 38.11, 44.27, 64.22, and 77.47°, corresponding to (111), (200), (220), and (311) planes, respectively [41].

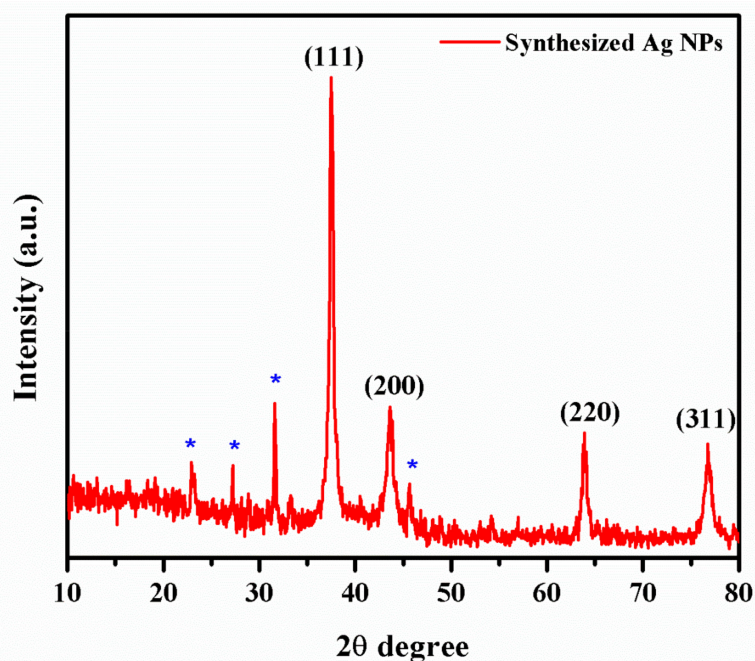


Figure 4. XRD analysis of Ag NPs.

3.4. SEM, TEM, and Selected Area Electron Diffraction (SAED) Analysis of Ag NPs

The surface morphology of the synthesized Ag NPs was studied by SEM analysis (Figure 5a,b). The SEM images illustrated agglomerated spherical-shaped nanoparticles with sizes in the range of 50 nm [42]. The crystallographic structure and accurate particle size of the Ag NPs were determined by the TEM analysis. The Ag NPs showed spherical morphology with sizes ranging from 35 to 50 nm, as shown in Figure 6a–c [42].

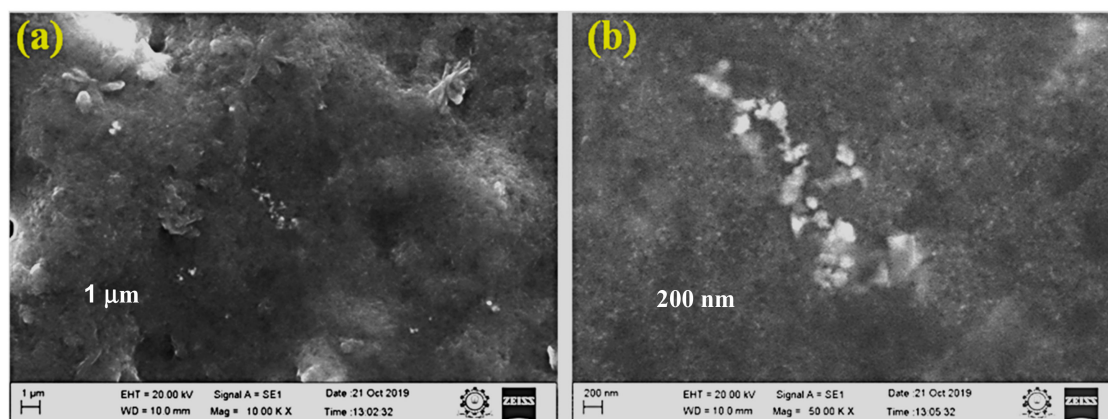


Figure 5. (a,b) SEM image of Ag NPs.

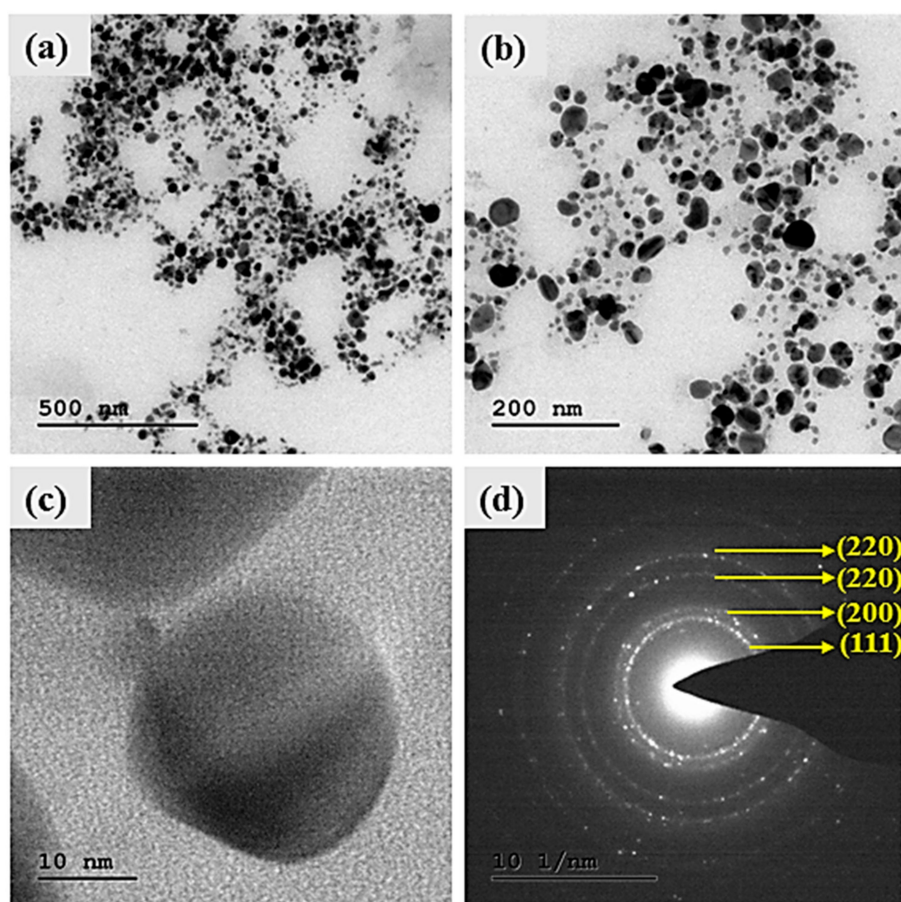


Figure 6. TEM image: (a) 500 nm, (b) 200 nm, (c) 10 nm, and (d) selected area diffraction electron (SAED) patterns of Ag NPs synthesized from *S. irio*.

3.5. Antibacterial Activity

The antibiotic-resistant characteristics of *P. aeruginosa* and *A. baumannii*, which cause ventilator-associated pneumonia, and the reference strain ATCC *E. coli*-25922 are shown in Table 1. From the results, it was observed that *P. aeruginosa* and *A. baumannii* exhibit similar resistance characteristics against the tested antibiotics (resistant to nine antibiotics and susceptible to four antibiotics). The reference strain ATCC *E. coli*-25922 was susceptible to the entire list of antibiotics as expected. In order to evaluate the antibacterial activity, different concentrations (6.25, 12.5, 25, 50, and 100 μg) of the synthesized Ag NPs were tested against MDR *P. aeruginosa*, *A. baumannii*, and ATCC *E. coli*-25922 by the well diffusion method (Table 2). All the tested concentrations exhibited the zone of inhibition and the antibacterial activity increased with an increase in the concentration of Ag NPs, which proves a dose-dependent response (Figure 7). Among them, the 100- μg concentration showed excellent antibacterial activity on *P. aeruginosa*, followed by *A. baumannii* and ATCC *E. coli*-25922.

Table 1. The antimicrobial-resistant pattern of selected multidrug-resistant pathogens.

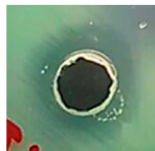
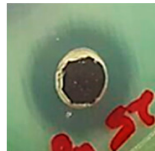
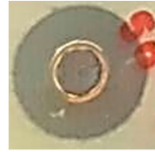
Antibiotics Group	Concentration (μg)	<i>P. aeruginosa</i>	<i>A. baumannii</i>	<i>E. coli</i> (ATCC: 25922)
Aminoglycosides				
Amikacin (AN)	8; 16; 64	R*	R	S**
Gentamicin (GM)	4; 16; 32	R	R	S
Tobramycin (TM)	8; 16; 64	R	R	S

Table 1. Cont.

Antibiotics Group	Concentration (µg)	<i>P. aeruginosa</i>	<i>A. baumannii</i>	<i>E. coli</i> (ATCC: 25922)
Carbapenems				
Ertapenem (ETP)	0.1; 6	S	S	S
Imipenem (IPM)	1; 2; 6; 12	S	S	S
Meropenem (MEM)	0.5,2,6,12	S	S	S
Cephalosporins				
Ceftazidime (CAZ)	1; 2; 8; 32	R	R	S
Cefepime (FEP)	2; 8; 26; 32	R	R	S
Fluoroquinolones				
Ciprofloxacin (CIP)	0.5; 2; 4	R	R	S
Levofloxacin (LEV)	0.25; 0.5; 2; 8	R	R	S
Tetracyclines				
Tigecycline	0.75; 2; 4	R	R	S
Polypeptides				
Colistin (CS)	4; 16; 32	S	S	S
Co-Trimoxazole				
Trimethoprim/Sulphonamides	1/19; 4/76; 16/304	R	R	S

R*: Resistant; S*: Susceptible. Organisms and their multidrug-resistant characteristics were studied using the GN: 21341 card and AST-N 292 card of the VITEK 2 automated system, respectively. (BioMérieux, Durham, USA). The antimicrobial susceptibility pattern was interpreted as per the European Committee on Antimicrobial Susceptibility Testing (EUCAST) recommendations (<http://www.eucastr.org/clinicalbreakpoints>).

Table 2. Antibacterial activities of the synthesized Ag NPs against *P. aeruginosa*, *A. baumannii*, and *E. coli*.

Organism	Concentration of Ag NPS					Meropenem (10 µg)
	6.25 µg	12.5 µg	25 µg	50 µg	100 µg	
Antibacterial Effect Against VAP Causing MDR Pathogens and Reference Strains						
<i>P. aeruginosa</i>						
<i>A. baumannii</i>						
<i>E. coli</i> (ATCC-25922)						

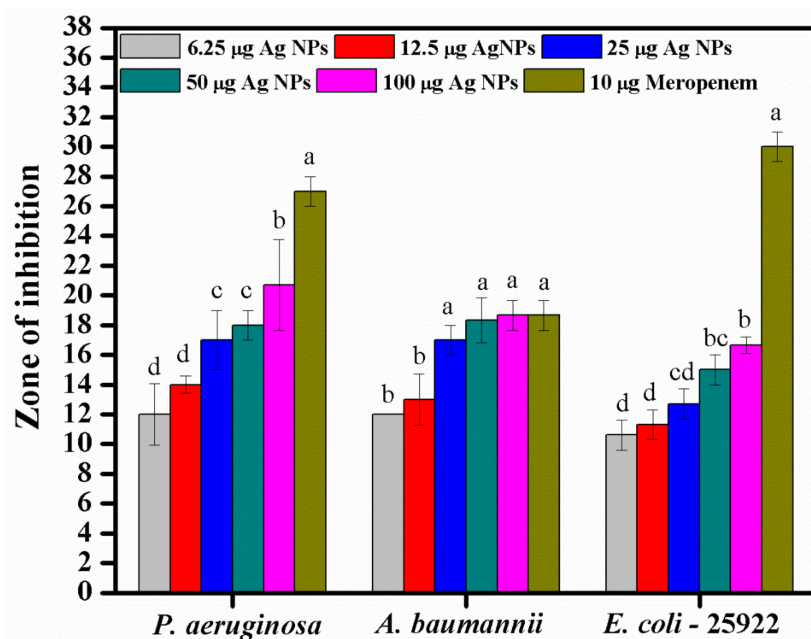


Figure 7. Antibacterial activities of the synthesized Ag NPs and the standard antibiotic Meropenem (10 µg) against ventilator-associated pneumoniae causing multidrug-resistant gram-negative clinical pathogens with the reference strain ATCC *E. coli*-25922. The T-bars represent standard errors. The different small alphabet letters above each column indicate significant differences (ANOVA, Tukey's HSD test, $p \leq 0.05$).

4. Discussion

In the synthesis of Ag NPs using the selected seasonal desert plant leaves, a slow visual color change from colorless to brown was observed. This color change confirmed the reduction of Ag^+ into Ag^0 . The UV-vis spectrum of the mixture at this stage showed a strong absorption peak at 426 nm corresponding to the wavelength of the surface plasmon resonance (SPR) of Ag NPs. SPR is a collective oscillation of conduction band electrons in metal nanoparticles under the influence of excited electromagnetic incident light. The SPR band is used to determine the nanoparticle size and geometry. A blue shift indicates a decrease in the particle size, while a redshift reveals an increase in the particle size. The rapid reduction process depends on the content of bioactive phytoconstituents, pH and temperature. This trend is well-consistent with earlier research [43–47].

In FTIR spectrum of *S. irio* leaf extract, the bands observed at 602 cm^{-1} and 508 cm^{-1} were due to the bending vibrations of N–H groups in proteins and C–Cl stretching, respectively. The functional groups indicated the presence of primary bioactive phytochemicals, such as glycosides, triterpenes, amino acids, coumarin, tannins, flavonoids, alkaloids, and saponins [20,21], in the *S. irio* leaf extract. Remarkably, a new band was observed at 1337 cm^{-1} in the spectrum of the synthesized Ag NPs corresponding to C–O stretching mode, which indicated the reduction of Ag^+ ions to Ag^0 NPs [38–40]. In turn, the transparency of synthesized Ag NPs decreased to a small extent when compared the leaf extract, which also indicated the reduction of the metal ions to metal nanoparticles. Our results showed good correlation with a previous report [1].

In the powder XRD pattern, there were four intense peaks at angles (2θ) 38.11, 44.27, 64.22, and 77.47° , corresponding to (111), (200), (220), and (311) planes, respectively. All reflections can be indexed to the face-centered cubic nature of synthesized Ag NPs. The characteristic peak values were confirmed by the Joint Committee on Powder Diffraction Standards (JCPDS File No: 04-0783). Some of the unassigned peaks observed in the XRD pattern were related to the phytochemicals present on the surface of Ag NPs. From the XRD data, the calculated average crystallite size was 21.59 nm. A similar observation has been made in recent studies [48–50].

The results of the SEM analysis showed the surface morphology of the synthesized Ag NPs to be agglomerated spherical-shaped with sizes ranging up to 50 nm. The TEM analysis revealed the spherical appearance of Ag NPs with sizes ranging from 35 nm to 50 nm. The particles were uniformly distributed without any aggregation. These results correlated and were in well-agreement with previous studies [43,51,52]. The selected area electron diffraction (SAED) pattern showed well-defined, spotty rings, implying the polycrystalline nature of the nanoparticles, which well-matched with the XRD results, as shown in Figure 6d. The d-spacing values were calculated using the following equation [53]:

$$L\lambda = dR \quad (1)$$

According to the literature, antibiotic development continues to stagnate. There has been no new class of antibiotics discovered since 1987 for the treatment of MDR pathogens inclusive of systemic gram-negative bacterial infections. Further, the World Health Organization (WHO) published a list of antibiotic-resistant bacteria as “Priority pathogens”, which need new antibiotics urgently [54]. The Ag NPs synthesized in this study using *S. irio* leaves proved potential antibacterial efficacy against the selected intrinsic MDR pathogens. The antimicrobial-resistant characteristics of *P. aeruginosa* and *A. baumannii* was assessed by the VITEK-2 automated system. On the other hand, the reference strain ATCC *E. coli*-25922 was susceptible to the entire list of antibiotics as expected. A similar trend was reported by Nys et al. (2018) [55,56]. The inhibitory zones of *P. aeruginosa* were in accordance with the results reported by Singh et al. (2014) [40]. The authors synthesized Ag NPs from *Tinospora cordifolia*, which showed zones of inhibition ranging from 11 mm to 18 mm at the concentration of 100 µg/mL against 20 MDR *P. aeruginosa* strains. Green synthesized Ag NPs have been shown to be powerful antibacterial agents against MDR *P. aeruginosa* and *A. baumannii* by several authors [57–59]. The size and concentration of the nanoparticles play a key role in the antibacterial activity.

The exact mechanism of antibacterial activity of the Ag NPs remains unclear. However, acceptable mechanisms have been proposed in the literature as follows: Ag NPs come into contact with the negatively charged bacterial cell membrane by an electrostatic interaction, leading to the disorganization of the membrane permeability and leakage of bacterial electrolyte, thus causing damages to the structure and function of mesosomes. The silver nanoparticles react with sulfhydryl (-SH) groups inside the cytosol, inactivate the protein synthesis, and suppress the activity of the enzyme. The interference with the intracellular cell signaling reduces the ATP synthesis, which increases the ROS generation and causes cell death [1,16,20].

5. Conclusions

A simple and rapid method for the synthesis of Ag NPs using leaf extract *S. irio* at room temperature (27 °C) without any chemicals was devised. The synthesized Ag NPs were thoroughly studied for their physicochemical properties. The antibacterial activity of the nanoparticles against MDR nosocomial pathogens causing ventilator-associated pneumonia (VAP) was investigated in detail. The Ag NPs potentially inhibited the selected pathogens even at the lowest concentration. The UV-vis spectrum revealed an absorbance band at 426 nm that confirmed the reduction of Ag⁺ metal ions to Ag⁰ NPs. In the FTIR spectrum of the Ag NPs, a new vibration band at 1337 cm⁻¹ corresponding to -C-O stretching appeared due to the reduction influence of glycosides and tannins. At the same time, the transparency of Ag NPs decreased when compared to that of the pure leaf extract. The powder XRD studies showed that the Ag NPs had a face-centered cubic structure with good crystalline nature. The surface morphology of the synthesized Ag NPs exhibited a spherical shape with sizes ranging from 35 to 50 nm. The antibacterial activity of the Ag NPs showed a dose-dependent response. The lowest concentration used in this study, 6.25 µg, effectively inhibited the intrinsic MDR pathogens *P. aeruginosa* and *A. baumannii*. In accordance with the present situation, there is an urgent need to decrease the burden of existing antibiotics and slow down the development of antibiotic resistance through an alternative method. Therefore, the synthesized Ag NPs gained the attention of many researchers. Silver nanoparticles may find applications in various hospital-associated surgical accessories, catheters,

wound-healing fabric dressings, antimicrobial papers, and as an additive in pharmaceutical products to reduce and manage the MDR bacterial infections and spread.

Author Contributions: The author designed the project and carried out the research work with the Majmaah University individual grant research approval. The author written the manuscript and critically revised.

Funding: The author thankful to the Basic Science Research Unit, Deanship of Scientific Research, Majmaah University, Kingdom of Saudi Arabia (Project Grant No: 38/63, signed dated: 11/12/1439H) for funding this research.

Acknowledgments: I gratefully acknowledge and thank all who gave all the technical support and Department of Biology, College of Science, Majmaah University, Al Zulfi, Kingdom of Saudi Arabia.

Conflicts of Interest: The authors have no conflicts of interest to declare.

References

1. Al-Ansari, M.; Alkubaisi, N.; Gopinath, K.; Karthika, V.; Arumugam, A.; Govindarajan, M. Facile and Cost-Effective Ag Nanoparticles Fabricated by *Lilium lancifolium* Leaf Extract: Antibacterial and Antibiofilm Potential. *J. Clust. Sci.* **2019**, *30*, 1081–1089. [[CrossRef](#)]
2. Huang, H.; Yang, X. Synthesis of polysaccharide-stabilized gold and silver nanoparticles: A green method. *Carbohydr. Res.* **2004**, *339*, 2627–2631. [[CrossRef](#)] [[PubMed](#)]
3. Vinod, V.T.P.; Saravanan, P.; Sreedhar, B.; Devi, D.K.; Sashidhar, R.B. A facile synthesis and characterization of Ag, Au and Pt nanoparticles using a natural hydrocolloid gum kondagogu (*Cochlospermum gossypium*). *Colloid. Surfaces B.* **2011**, *83*, 291–298. [[CrossRef](#)] [[PubMed](#)]
4. Kumar, K.M.; Mandal, B.K.; Kumar, K.S.; Reddy, P.S.; Sreedhar, B. Biobased green method to synthesise palladium and iron nanoparticles using *Terminalia chebula* aqueous extract. *Spectrochim. Acta A.* **2013**, *102*, 128–133. [[CrossRef](#)] [[PubMed](#)]
5. Yuan, Z.; Li, R.; Meng, F.; Zhang, J.; Zuo, K.; Han, E. Approaches to Enhancing Gas Sensing Properties: A Review. *Sensors* **2019**, *19*, 1495. [[CrossRef](#)] [[PubMed](#)]
6. Rajaei, E.; Ravandi, S.A.H.; Valipouri, A. Electrochemical and photovoltaic properties of dye-sensitized solar cells based on Ag-doped TiO₂ nanorods. *Optik* **2018**, *158*, 514–521. [[CrossRef](#)]
7. Rehan, M.; Mashaly, H.M.; Mowafi, S.; El-Kheir, A.A.; Emam, H.E. Multi-functional textile design using in-situ Ag NPs incorporation into natural fabric matrix. *Dyes Pigments.* **2015**, *118*, 9–17. [[CrossRef](#)]
8. Zhang, Y.; Wang, L.; Kong, X.; Jiang, H.; Zhang, F.; Shi, J. Novel Ag-Cu bimetallic alloy decorated near-infrared responsive three-dimensional rod-like architectures for efficient photocatalytic water purification. *J. Colloid Interf. Sci.* **2018**, *522*, 29–39. [[CrossRef](#)]
9. Sallum, L.F.; Soares, F.L.F.; Ardila, J.A.; Carneiro, R.L. Optimization of SERS scattering by Ag-NPs-coated filter paper for quantification of nicotinamide in a cosmetic formulation. *Talanta* **2014**, *118*, 353–358. [[CrossRef](#)]
10. Sarwar, M.S.; Niazi, M.B.K.; Jahan, Z.; Ahmad, T.; Hussain, A. Preparation and characterization of PVA/nanocellulose/Ag nanocomposite films for antimicrobial food packaging. *Carbohydr. Polym.* **2018**, *184*, 453–464. [[CrossRef](#)]
11. Anandan, M.; Poorani, G.; Boomi, P.; Varunkumar, K.; Anand, K.; Chaturgoon, A.A.; Saravanan, M.; Prabu, H.G. Green synthesis of anisotropic silver nanoparticles from the aqueous leaf extract of *Dodonaea viscosa* with their antibacterial and anticancer activities. *Process Biochem.* **2019**, *80*, 80–88. [[CrossRef](#)]
12. Alharbi, N.S.; Govindarajan, M.; Kadaikunnan, S.; Khaled, J.M.; Almanaa, T.N.; Alyahya, S.A.; Al-Anbr, M.N.; Gopinath, K.; Sudha, A. Nanosilver crystals capped with *Bauhinia acuminata* phytochemicals as new antimicrobials and mosquito larvicides. *J. Trace Elem. Med. Bio.* **2018**, *50*, 146–153. [[CrossRef](#)] [[PubMed](#)]
13. Bello, B.A.; Khan, S.A.; Khan, J.A.; Syed, F.Q.; Mirza, M.B.; Shah, L.; Khan, S.B. Anticancer, antibacterial and pollutant degradation potential of silver nanoparticles from *Hyphaene thebaica*. *Biochem. Bioph. Res. Co.* **2017**, *490*, 889–894. [[CrossRef](#)] [[PubMed](#)]
14. Hebbalalu, D.; Lalley, J.M.; Nadagouda, N.; Varma, R.S. Greener Techniques for the Synthesis of Silver Nanoparticles Using Plant Extracts, Enzymes, Bacteria, Biodegradable Polymers, and Microwaves. *ACS Sustain. Chem. Eng.* **2013**, *1*, 703–712. [[CrossRef](#)]
15. Kuppusamy, P.; Yusoff, M.M.; Maniam, G.P.; Govindan, N. Biosynthesis of metallic nanoparticles using plant derivatives and their new avenues in pharmacological applications—An updated report. *Saudi Pharm. J.* **2016**, *24*, 473–484. [[CrossRef](#)] [[PubMed](#)]

16. Gopinath, K.; Kumaraguru, S.; Bhakayaraj, K.; Mohan, S.; Venkatesh, K.S.; Esakkirajan, M.; Kaleeswarran, P.; Alharbi, N.S. Green synthesis of silver, gold and silver/gold bimetallic nanoparticles using the *Gloriosa superba* leaf extract and their antibacterial and antibiofilm activities. *Micro. Pathog.* **2016**, *101*, 1–11. [[CrossRef](#)] [[PubMed](#)]
17. Pirtarighat, S.; Ghannadnia, M.; Baghshahi, S. Green synthesis of silver nanoparticles using the plant extract of *Salvia spinosa* grown in vitro and their antibacterial activity assessment. *J. Nanostruct. Chem.* **2019**, *9*, 1–9. [[CrossRef](#)]
18. Prabakar, K.; Sivalingam, P.; Rabeek, S.I.M.; Muthuselvam, M.; Devarajan, N.; Arjunan, A.; Karthick, R.M.; Suresh, M.; Wembonyama, J.P. Evaluation of antibacterial efficacy of phyto fabricated silver nanoparticles using *Mukia scabrella* (Musumusukkai) against drug resistance nosocomial gram negative bacterial pathogens. *Colloid. Surface B.* **2013**, *104*, 282–288. [[CrossRef](#)]
19. Yugandhar, P.; Savithamma, N. Biosynthesis, characterization and antimicrobial studies of green synthesized silver nanoparticles from fruit extract of *Syzygium alternifolium* (Wt.) Walp. an endemic, endangered medicinal tree taxon. *Appl. Nanosci.* **2016**, *6*, 223–233. [[CrossRef](#)]
20. Al-Jaber, N.A. Phytochemical and biological studies of *Sisymbrium irio* L. Growing in Saudi Arabia. *J. Saudi Chem. Soc.* **2011**, *15*, 345–350. [[CrossRef](#)]
21. Al-Massarani, S.M.; El-Gamal, A.A.; Alam, P.; Al-Sheddi, E.S.; Al-Oqail, M.M.; Farshori, N.N. Isolation, biological evaluation and validated HPTLC-quantification of the marker constituent of the edible Saudi plant *Sisymbrium irio* L. *S. Pharm. J.* **2017**, *25*, 750–759. [[CrossRef](#)] [[PubMed](#)]
22. Jeyaseelan, S.; Revathi, P.; Rath, P.K.; Suresh, M.; Vigeneshwari, R.S.; Uma, A.; Subramanian, P.T.K.; Moorthy, K.; Thajuddin, N. Antimicrobial Resistant Pattern of Gram Negative Bacteria to Third Generation Cephalosporins in Rural and Urban Centres of Tamil nadu, India. *Int. J. Biological. Tech.* **2012**, *3*, 32–38.
23. Kannaiyan, M.; Manuel, V.N.; Raja, V.; Thambidurai, P.; Mickymaray, S.; Nooruddin, T. Antimicrobial activity of the ethanolic and aqueous extracts of *Salacia chinensis* Linn. against human pathogens. *Asian Pac. J. Trop. Dis.* **2012**, *2*, 416–420. [[CrossRef](#)]
24. Mickymaray, S.; Alturaiki, W.; Al-Aboody, M.S.; Mariappan, P.; Rajenderan, V.; Alsagaby, S.A.; Kalyanasundram, U.; Alarfajj, A.A. Anti-bacterial efficacy of bacteriocin produced by marine *Bacillus subtilis* against clinically important extended spectrum beta-lactamase strains and methicillin-resistant *Staphylococcus aureus*. *Int. J. Med. Res. Health Sci.* **2018**, *7*, 75–83.
25. Mickymaray, S.; Alturaiki, W. Antifungal efficacy of marine macroalgae against fungal isolates from bronchial asthmatic cases. *Molecules* **2018**, *23*, 3032. [[CrossRef](#)]
26. Mickymaray, S.; Al Aboody, M.S. In Vitro Antioxidant and Bactericidal Efficacy of 15 Common Spices: Novel Therapeutics for Urinary Tract Infections? *Medicina* **2019**, *55*, 289. [[CrossRef](#)]
27. Saranya, A.S.; Suresh, M.; Al Aboody, M.S.; Rath, P.K.; Kibemo, B.; Kannaiyan, M. Prevalence of metallo β -lactamases in carbapenem resistant *Acinetobacter baumannii* isolated from tracheal secretions. *Int. J. Recent Sci. Res.* **2017**, *8*, 15197–15202.
28. Falagas, M.E.; Tansarli, G.S.; Karageorgopoulos, D.E.; Vardakas, K.Z. Deaths Attributable to Carbapenem-Resistant *Enterobacteriaceae* Infections. *Emerg. Infect. Dis.* **2014**, *20*, 1170. [[CrossRef](#)]
29. Lemos, E.V.; de La Hoz, F.P.; Einarson, T.R.; McGhan, W.F.; Quevedo, E.; Castaneda, C.; Kawai, K. Carbapenem resistance and mortality in patients with *Acinetobacter baumannii* infection: Systematic review and meta-analysis. *Clin. Microbiol. Infec.* **2014**, *20*, 416–423. [[CrossRef](#)]
30. Shamsizadeh, Z.; Nikaeen, M.; Esfahani, B.N.; Mirhoseini, S.H.; Hatamzadeh, M.; Hassanzadeh, A. Detection of antibiotic resistant *Acinetobacter baumannii* in various hospital environments: Potential sources for transmission of *Acinetobacter* infections. *Environ. Health Prev.* **2017**, *22*, 44. [[CrossRef](#)]
31. Fournier, P.E.; Richet, H.; Weinstein, R.A. The Epidemiology and Control of *Acinetobacter baumannii* in Health Care Facilities. *Clin. Infect. Dis.* **2006**, *42*, 692–699. [[CrossRef](#)] [[PubMed](#)]
32. Kilic, A.; Li, H.; Mellmann, A.; Basustaoglu, A.C.; Kul, A.C.; Senses, Z.; Aydogan, H.; Stratton, C.W.; Harmsen, D.; Tang, Y.W. *Acinetobacter septicus* sp. nov. Association with a Nosocomial Outbreak of Bacteremia in a Neonatal Intensive Care Unit. *J. Clin. Microbio.* **2008**, *46*, 902–908. [[CrossRef](#)] [[PubMed](#)]
33. Mickymaray, S.; Al Aboody, M.S.; Rath, P.K.; Annamalai, P.; Nooruddin, T. Screening and antibacterial efficacy of selected Indian medicinal plants. *Asian Pac. J. Trop. Biomed.* **2016**, *6*, 185–191. [[CrossRef](#)]

34. Lim, S.S.; Selvaraj, A.; Ng, Z.Y.; Palanisamy, M.; Mickymaray, S.; Cheong, P.C.H.; Lim, R.L.H. Isolation of actinomycetes with antibacterial activity against multi-drug resistant bacteria. *Malays. J. Microbiol.* **2018**, *14*, 293–305.
35. Gopinath, K.; Gowri, S.; Arumugam, A. Phytosynthesis of silver nanoparticles using *Pterocarpus santalinus* leaf extract and their antibacterial properties. *J. Nanostruct. Chem.* **2013**, *3*, 68. [[CrossRef](#)]
36. Krishnaraj, C.; Ramachandran, R.; Mohan, K.; Kalaichelvan, P.T. Optimization for rapid synthesis of silver nanoparticles and its effect on phytopathogenic fungi. *Spectrochim. Acta A.* **2012**, *93*, 95–99. [[CrossRef](#)] [[PubMed](#)]
37. Perez, C. Antibiotic assay by agar-well diffusion method. *Acta Biol. Med. Exp.* **1990**, *15*, 113–115.
38. Jayaseelan, C.; Rahuman, A.A.; Rajakumar, G.; Kirthi, A.V.; Santhoshkumar, T.; Marimuthu, S.; Bagavan, A.; Kamaraj, C.; Zahir, A.A.; Elango, G. Synthesis of pediculocidal and larvicidal silver nanoparticles by leaf extract from heartleaf moonseed plant, *Tinospora cordifolia* Miers. *Parasitol. Res.* **2011**, *109*, 185–194. [[CrossRef](#)]
39. Anuj, S.A.; Ishnava, K.B. Plant mediated synthesis of silver nanoparticles by using dried stem powder of *Tinospora cordifolia*, its antibacterial activity and comparison with antibiotics. *Int. J. Pharma. Biol. Sci.* **2013**, *4*, 849–863.
40. Singh, K.; Panghal, M.; Kadyan, S.; Chaudhary, U.; Yadav, J.P. Antibacterial Activity of Synthesized Silver Nanoparticles from *Tinospora cordifolia* against Multi Drug Resistant Strains of *Pseudomonas aeruginosa* Isolated from Burn Patients. *J. Nanomed. Nanotechnol.* **2014**, *5*, 192. [[CrossRef](#)]
41. López-Miranda, J.L.; Vázquez, M.; Fletes, N.; Esparza, R.; Rosas, G. Biosynthesis of silver nanoparticles using a *Tamarix gallica* leaf extract and their antibacterial activity. *Mater. Lett.* **2016**, *176*, 285–289. [[CrossRef](#)]
42. Ravichandran, V.; Vasanthi, S.; Shalini, S.; Shah, S.A.A.; Harish, R. Green synthesis of silver nanoparticles using *Atrocarpus altilis* leaf extract and the study of their antimicrobial and antioxidant activity. *Mater. Lett.* **2016**, *180*, 264–267. [[CrossRef](#)]
43. Krishnaraj, C.; Jagan, E.G.; Rajasekar, S.; Selvakumar, P.; Kalaichelvan, P.T.; Mohan, N. Synthesis of silver nanoparticles using *Acalypha indica* leaf extracts and its antibacterial activity against water borne pathogens. *Colloid. Surface. B.* **2010**, *76*, 50–56. [[CrossRef](#)] [[PubMed](#)]
44. Rajeshkumar, S.; Kannan, C.; Annadurai, G. Synthesis and Characterization of Antimicrobial Silver Nanoparticles Using Marine Brown Seaweed *Padina tetrastrum*. *Drug Invent. Today.* **2012**, *4*, 511–513.
45. Durán, N.; Marcato, P.D.; De Souza, G.I.; Alves, O.L.; Esposito, E. Antibacterial Effect of Silver Nanoparticles Produced by Fungal Process on Textile Fabrics and Their Effluent Treatment. *J. Biomed. Nanotechnol.* **2007**, *3*, 203–208. [[CrossRef](#)]
46. Umashankari, J.; Inbakandan, D.; Ajithkumar, T.T.; Balasubramanian, T. Mangrove plant, *Rhizophora mucronata* (Lamk, 1804) mediated one pot green synthesis of silver nanoparticles and its antibacterial activity against aquatic pathogens. *Aquat. Biosyst.* **2012**, *8*, 11. [[CrossRef](#)]
47. Vanaja, M.; Annadurai, G. *Coleus aromaticus* leaf extract mediated synthesis of silver nanoparticles and its bactericidal activity. *Appl. Nanosci.* **2013**, *3*, 217–223. [[CrossRef](#)]
48. Chowdhury, S.; Basu, A.; Kundu, S. Green synthesis of protein capped silver nanoparticles from phytopathogenic fungus *Macrophomina phaseolina* (Tassi) Goid with antimicrobial properties against multidrug-resistant bacteria. *Nanoscale Res. Lett.* **2014**, *9*, 365. [[CrossRef](#)]
49. Anandalakshmi, K.; Venugobal, J.; Ramasamy, V. Characterization of silver nanoparticles by green synthesis method using *Pedaliium murex* leaf extract and their antibacterial activity. *Appl. Nanosci.* **2016**, *6*, 399–408. [[CrossRef](#)]
50. Jyoti, K.; Baunthiyal, M.; Singh, A. Characterization of silver nanoparticles synthesized using *Urtica dioica* Linn. leaves and their synergistic effects with antibiotics. *J. Radiat. Res. Appl. Sci.* **2016**, *9*, 217–227. [[CrossRef](#)]
51. Behravan, M.; Panahi, A.H.; Naghizadeh, A.; Ziaee, M.; Mahdavi, R.; Mirzapour, A. Facile green synthesis of silver nanoparticles using *Berberis vulgaris* leaf and root aqueous extract and its antibacterial activity. *Int. J. Bio. Macromol.* **2019**, *124*, 148–154. [[CrossRef](#)] [[PubMed](#)]
52. Mittal, A.K.; Chisti, Y.; Banerjee, U.C. Synthesis of metallic nanoparticles using plant extracts. *Biotechnol. Adv.* **2013**, *31*, 346–356. [[CrossRef](#)] [[PubMed](#)]
53. Xu, Z.; He, L.; Mu, R.; Zhong, X.; Cao, X. Formation of diffusion barrier on the Ni-based superalloy by low-pressure pre-oxidation. *Vacuum* **2008**, *82*, 1251–1258. [[CrossRef](#)]

54. WHO Publishes List of Bacteria for Which New Antibiotics are Urgently Needed. Geneva. Available online: <http://www.who.int/mediacentre/news/releases/2017/bacteria-antibiotics-needed/en/> (accessed on 26 September 2019).
55. Nys, S.; Terporten, P.H.; Korstanje, J.A.A.H.; Stobberingh, E.E. Trends in antimicrobial susceptibility of *Escherichia coli* isolates from urology services in the Netherlands (1998–2005). *J. Antimicrob Chemother* **2008**, *62*, 126–132. [[CrossRef](#)]
56. Vijayakumar, R.; Sandle, T.; Al-Aboody, M.S.; AlFonaisan, M.K.; Alturaiki, W.; Mickymaray, S.; Premanathan, M.; Alsagaby, S.A. Distribution of biocide resistant genes and biocides susceptibility in multidrug-resistant *Klebsiella pneumoniae*, *Pseudomonas aeruginosa* and *Acinetobacter baumannii*—A first report from the Kingdom of Saudi Arabia. *J. Infect. Public Health*. **2018**, *11*, 812–816. [[CrossRef](#)]
57. Chen, M.; Yu, X.; Huo, Q.; Yuan, Q.; Li, X.; Xu, C.; Bao, H. Biomedical Potentialities of Silver Nanoparticles for Clinical Multiple Drug-Resistant *Acinetobacter baumannii*. *J. Nanomater.* **2019**, *2019*, 7. [[CrossRef](#)]
58. Jinu, U.; Jayalakshmi, N.; Anbu, A.S.; Mahendran, D.; Sahi, S.; Venkatachalam, P. Biofabrication of Cubic Phase Silver Nanoparticles Loaded with Phytochemicals from *Solanum nigrum* Leaf Extracts for Potential Antibacterial, Antibiofilm and Antioxidant Activities Against MDR Human Pathogens. *J. Clust. Sci.* **2017**, *28*, 489–505. [[CrossRef](#)]
59. Kasithevar, M.; Periakaruppan, P.; Muthupandian, S.; Mohan, M. Antibacterial efficacy of silver nanoparticles against multi-drug resistant clinical isolates from post-surgical wound infections. *Micro. Pathog.* **2017**, *107*, 327–334. [[CrossRef](#)]



© 2019 by the author. Licensee MDPI, Basel, Switzerland. This article is an open access article distributed under the terms and conditions of the Creative Commons Attribution (CC BY) license (<http://creativecommons.org/licenses/by/4.0/>).